Published in final edited form as:
Invest Ophthalmol Vis Sci. 2005 September ; 46(9): 3197–3207.

Structure–Function Relations of Parasol Cells in the Normal and Glaucomatous Primate Retina

Arthur J. Weber[1,2] and **Christine D. Harman**[1]
1*From the Department of Physiology and the*

2*Neuroscience Program, Michigan State University, East Lansing, Michigan.*

Abstract

Purpose—The purpose of this study was to examine the effect that chronic elevation of intraocular pressure has on the intrinsic and visual response properties of parasol cells in the primate retina.

Methods—A primate model of experimental glaucoma was combined with intracellular recording and staining techniques using an isolated retina preparation. Intrinsic electrical properties were examined by injection of depolarizing and hyperpolarizing currents. Visual responses were studied using drifting and counterphased gratings. Morphologic comparisons were made by injecting recorded cells with Neurobiotin and analyzing them quantitatively with a computer-based neuron reconstruction system.

Results—Structurally, parasol cells from glaucomatous eyes had smaller somata and smaller, less complex dendritic arbors, resulting in a significant reduction in total dendrite length and surface area. Functionally, these neurons did not differ from normal in their mean resting membrane potentials, input resistances, or thresholds to electrical activation, but did differ in membrane time constants and spike duration. Parasol cells from both normal and glaucomatous eyes preferred low-spatial-frequency stimuli, but significantly fewer glaucoma-related cells were driven visually—in particular, by patterned stimuli. Glaucomatous cells also did not respond as well to visual stimuli presented at increased temporal frequencies.

Conclusions—Ganglion cells in the glaucomatous eye retain most of their normal intrinsic electrical properties, but are less responsive, both spatially and temporally, to visual stimuli. The reduction in visual responsiveness most likely results from significant changes in dendritic architecture, which affects their level of innervation by more distal retinal neurons.

Primary open-angle glaucoma is a leading cause of blindness often characterized by an elevation of intraocular pressure (IOP). The disease process is thought to originate at the level of the lamina cribrosa within the optic nerve head, where exiting retinal ganglion cell axons are subjected to mechanical, vascular, and/or biochemical injury as a result of the increased IOP.[1–7]

Over the past several years, a number of studies have described the degenerative effects that chronic elevation of IOP and glaucoma have on fibers in the optic nerve, as well as the concomitant loss of ganglion cells that occurs within the retina itself.[8–10] More recently, we combined the monkey model of experimental glaucoma with intracellular staining techniques to examine the pattern of degenerative changes that characterize glaucomatous neuropathy at the single cell level.[11] The results of these studies indicate that in both midget and parasol

Corresponding author: Arthur J. Weber, Department of Physiology, 2193 Biomedical and Physical Sciences Building, Michigan State University, East Lansing, MI 48824;weberar@msu.edu..

Disclosure: **A.J. Weber**, None; **C.D. Harman**, None

Supported by National Eye Institute Grant EY11159 (AJW).

cells, structural abnormalities at the level of the dendritic arbor represent the earliest signs of glaucoma-related retinal ganglion cell degeneration. These changes include a thinning of both proximal and distal dendritic processes, abrupt changes in dendrite thickness at branch points, and a general reduction in dendritic arbor complexity. Reductions in soma size and proximal axon diameter also occur, albeit slightly later in the degenerative process.

Because retinal ganglion cells receive all their input from more distal retinal elements through their dendrites,[12,13] abnormalities in dendritic structure suggest a reduction in synaptic efficacy, and early functional deficits at the single-cell level. The primary goal of the present studies was, using parasol cells as the example, to determine the extent to which glaucoma-related changes in ganglion cell structure might also involve changes in the biophysical and visual response properties of single ganglion cells, thus indicating glaucoma-related visual dysfunction in advance of actual ganglion cell loss.

Methods

General Procedures

The data presented herein were obtained from 23 rhesus monkeys (*Macaca mulatta*) of both sexes that ranged in age from 9 to 16 years. All had clinically normal-appearing eyes, as determined by slit lamp biomicroscopy, gonioscopy (OG3M-13 lens; Ocular Instruments, Bellevue, WA), and stereoscopic funduscopy (TRC-50; Topcon, Paramus, NJ), and all had baseline IOP, measured under ketamine HCl anesthesia with a hand-held tonometer (Tono-Pen XL; Medtronic, Minneapolis, MN) below 21 mm Hg (normal IOP for ketamine-anesthetized rhesus monkeys, 10–20 mm Hg). The eyes were treated with 0.5% proparacaine HCl (Alcaine; Alcon Laboratories, Fort Worth, TX) for all procedures involving contact with the cornea. For fundus photography, the pupils were dilated with 2.5% phenylephrine HCl (Mydfrin; Alcon) and 1% tropicamide HCl (Mydriacil; Alcon). All procedures were approved by the Animal Care Committee at Michigan State University, and all adhered to the ARVO Statement for the Use of Animals in Ophthalmic and Vision Research.

In all the experimental animals with glaucoma (Table 1), IOP was elevated by multiple injections of a sterile solution containing 3.6×10^5 latex microspheres (10 μm diameter, F-8836; Molecular Probes, Eugene, OR) into the anterior chamber of one eye.[14] The fellow eyes, and those of eight untreated animals, served as normal control samples. Typically, 8 to 10 injections were needed to achieve a sustained elevation of IOP, and the frequency and size of subsequent injections were made based on biweekly measurements of IOP and the history of the eye's responsiveness to the prior injections. All eyes were examined with the slit lamp before each injection. Fundus photographs were obtained every 3 to 4 weeks, depending on the clinical appearance of the optic disc compared with its appearance during the previous eye examination.

After periods of elevated IOP that ranged from 18 to 144 weeks (Table 1), the animals were anesthetized deeply with ketamine HCl (15 mg/kg, intramuscularly) and pentobarbital sodium (35 mg/kg, intravenously). The eyes then were removed quickly and placed into oxygenated artificial cerebrospinal fluid (aCSF; pH 7.4),[15] the animal received an overdose of pentobarbital sodium and was perfused transcardially with 0.5 L of 0.9% saline followed by 2 L of a 10% formol-saline solution.

In Vitro Procedures

Immediately on enucleation, the anterior segment of each eye was removed and the posterior eyecup placed in a solution of aCSF saturated with a mixture of 95% O_2 and 5% CO_2 at 22° C. Before recording, each eyecup was flatmounted, ganglion cell layer up, in a chamber

perfused with oxygenated aCSF (3–8 mL/min) at 36.5°C and allowed 30 minutes to acclimate in dim light. The chamber then was mounted on the stage of an upright microscope equipped with epifluorescence, and single ganglion cells, prestained with acridine orange (1 mM, A-6014; Sigma-Aldrich, St. Louis, MO), were targeted with a 40× water immersion objective with a working distance of 1.6 mm.[11]

Intracellular Recording and Labeling

Intracellular recordings were made using glass microelectrodes filled with 1 M potassium acetate, 2% Neurobiotin (SP-1120; Vector Laboratories, Burlingame, CA), and 0.2% pyranine (41218; Acros Organics, Fairlawn, NJ). The electrodes were beveled to a final impedance of 35 to 45 MΩ at 30 Hz. Recordings were made using a hydraulic microdrive, high-impedance intracellular amplifier (AxoClamp 2B) with bridge and current injection circuitry and software (pClamp6/8; Axon Instruments, Union City, CA). Neurobiotin was iontophoresed into cells with positive-current pulses (1–2 nA) of 100 to 200 ms duration, and labeled cells were revealed with an avidin biotin complex (ABC) kit (Vectastain, SK-4100; Vector Laboratories).

Biophysical Measurements

After optimal capacitance compensation, the extracellular response to a brief pulse of negative current (−1 nA/0.5 ms) was used to determine the response characteristic of each electrode. Typically, this yielded electrodes with time constants of 100 to 200 μs, considerably faster than those measured intracellularly (1–4 ms). Electrodes were used for only a single penetration and were discarded if the electrical characteristics changed during recording. Whole-cell input resistance (Rn) was determined from the slope of the I-V curve derived by delivering a series of hyperpolarizing current pulses (0 to −1 nA in 0.1-nA steps of 250-ms duration) through the recording electrode. Membrane time constants (τ_m) were derived by fitting a standard exponential to the voltage decay curve that resulted from application of a brief pulse of hyperpolarizing current (−1 nA, 0.5 ms). Thresholds and firing rates were determined by applying depolarizing current pulses (0 nA to +1 nA in 0.1-nA steps of 250-ms duration) through the recording electrode and measuring the onset of spike activity, as well as the maximum number of spikes per second.

Visual Stimulation

Visual stimuli included drifting and counterphased light and dark bars presented by a computer-driven image synthesizer (Picasso; Innisfree, Cambridge, MA) and a high-resolution CRT (model 608 w/P4 phosphor; Tektronics, Beaverton, OR) that was directed through the microscope camera port. The mean luminance of the monitor, as measured with a 1° luminance head (J1823; Tektronics) and a photometer (J17; Tektronics), was 40 cd/m^2 at 60% contrast. Delivering the stimulus through the camera port and 40× water-immersion objective needed to target single cells reduced the luminance to approximately 1 cd/m^2. Spatial frequencies of 0.08 to 3.6 cyc/deg, presented at temporal frequencies of 0.5 to 25 Hz (highest rate the image synthesizer could generate), were randomly interleaved, presented five times each, and the resultant binned visual responses averaged. Each trial included the presentation of a blank screen (0% contrast), which was used to correct for cell–cell differences in spontaneous activity. Ganglion cells were considered linear if they displayed a null point and nonlinear if they displayed a doubling response, when presented with the appropriate, sinusoidally modulated (2–4 Hz) grating.[16]

Cell Sampling, Mapping, Classification, and Analysis

Because the intracellular approach does not allow sampling of a large number of neurons over the entire retina, we focused on ganglion cells located in the superior and inferior regions of the midtemporal retina (4–8 mm from the fovea), the region considered clinically to be the

most vulnerable to pressure-induced degeneration.[17–19] We also focused on parasol cells, because of the greater ease of obtaining stable, long-term, recordings, their high-contrast gain,[20–21] and previous work suggesting that these neurons may be most susceptible in the glaucomatous eye[22–24] (but see Ref. 9). Individual cells, prestained with acridine orange, were selected randomly for analysis. Cells initially were identified anatomically by their large somata and phasic responses to a maintained visual stimulus; after injection, fixation, and processing, the labeled cells were confirmed as parasol cells by their characteristic dendritic morphologies.[11–13,16,25–28] Before in vitro sampling, a map was made of the retinal blood vessel pattern and the approximate location of each recorded neuron. After the recording and processing, the retinal outline, optic disc, fovea, and location of each injected neuron were mapped with a computer-based stage digitizing system (AccuStage, Shoreview, MN). Cells labeled intracellularly with Neurobiotin were matched with their physiological data, reconstructed, and analyzed quantitatively by microscope (FX-A; Nikon, Tokyo, Japan), with a 100× oil-immersion objective and morphometric software (Neurolucida and NeuroExplorer; MicroBrightField, Inc., Colchester, VT). Distribution-based comparisons were made with the Mann-Whitney test, whereas mean data comparisons (presented as the mean ± SE) were made with a two-tailed Student's *t*-test. All statistical comparisons were made by computer (SPSS software; SPSS, Chicago, IL), with $P = 0.05$ as the level of significance.

Results

Morphologic Properties

A total of 108 parasol cells were recorded, 64 from normal retinas and 44 from eyes with experimental glaucoma. Of these, 29 normal ganglion cells and 36 glaucomatous cells were judged to be labeled completely and thus were suitable for morphologic analysis. In agreement with previous studies, all the labeled cells showed the basic structural features characteristic of parasol cells. These included large somata, large, radially oriented dendritic arbors that originate from four to five primary dendrites, and relatively thick proximal axon segments.[11–13,16,25–28] As a group, however, the parasol cells from the glaucomatous eyes were both qualitatively and quantitatively different from those examined in normal eyes. Qualitatively, these neurons appeared to contain fewer dendritic processes, resulting in a less complex dendritic tree. In addition, individual dendrites often showed greater variation in thickness along their lengths (Fig. 1). These qualitative observations were confirmed quantitatively (Table 2). Although closely matched in retinal eccentricity (27/29 normal and 34/36 glaucomatous cells sampled were located 5 to 7 mm temporal to the fovea), the somata and dendritic arbors of parasol cells from the glaucomatous eyes were, on average, 18% and 26% smaller than normal, respectively (Figs. 2A, 2B). Further analysis of the dendritic trees of these neurons revealed a 29% reduction in total dendrite length (Fig. 2C) and a 48% reduction in dendrite surface area (Fig. 2D) when compared with normal. Although the reductions in soma size and surface area were not significant, those related to the morphologic features of the dendritic arbor were (Table 2; Fig. 2). The dendritic complexity of each injected cell then was examined by counting the number of dendritic processes associated with each cell, and by use of a Sholl analysis.[29] The dendritic counts indicated a significant reduction (21%) in the mean number of dendritic processes associated with the glaucomatous eye neurons (Table 2). For the Sholl analysis, using spheres with radii that ranged from 10 to 160 μm, spaced at 10-μm increments, the total number of sphere-dendrite intersections for the normal parasol cells averaged 234.2 ± 18.0/cell, whereas that for the glaucomatous parasol cells was significantly less, only 168.3 ± 13.4/cell. That much of the effect is related to more distal regions of the dendritic arbor is suggested by the bias toward more proximal radii in the intersection distribution curves for these neurons (Fig. 3).

Biophysical Properties

Comparisons of the intrinsic membrane properties of cells from normal and glaucomatous eyes suggested only minor differences (Table 3). Ganglion cells from both groups of eyes displayed resting membrane potentials of approximately −53 mV (range: 48–62 mV), as well as similar activation thresholds (~0.32 nA) after intracellular application of depolarizing current pulses (0–1 nA). Although they also showed similar whole cell input resistances (21.7 ± 1.5 MΩ vs. 22.5 ± 1.9 MΩ), the time constants of parasol cells from the glaucomatous eyes were, on average, significantly shorter than those recorded in normal parasol cells (2.2 ± 0.12 ms vs. 2.7 ± 0.14 ms, respectively). Similarly, although there was no difference in the mean spike amplitudes in these two populations of cells (~46 mV), spike duration (measured as spike width at half height) was significantly longer in the glaucomatous versus normal parasol cells (0.5 ± 0.02 ms vs. 0.43 ± 0.02 ms).

The maximum firing rate (spikes per second) for each neuron was determined by counting the number of spikes that occurred in response to electrical stimulation with a 1 nA, 250 ms duration depolarizing pulse. This level of stimulation was used because higher levels often were detrimental to cells from the glaucomatous eyes. Although the mean response of the normal cells to such electrical stimulation was considerably greater than that of the glaucomatous cells (108.1 spikes/s vs. 92.8 spikes/s), these values were not significantly different, in part, because most parasol cells from either group of animals could be divided into one of three general types, according to their response to injection of depolarizing current: (1) neurons that were extremely phasic, and only responded with a single spike, even at high levels of stimulation, (2) neurons that showed moderate responses at low levels of stimulation, but increased the firing rate with increased stimulus intensity, and (3) neurons that displayed very robust responses to low current levels and increased their firing rates proportionally with increased levels of stimulation (Fig. 4A–C, respectively). These response characteristics did not appear to be related to whether the cells displayed linear or nonlinear spatial summation or whether they were electrically coupled with other retinal neurons. Only four cells, all normal, showed coupling. Although the level of coupling ranged from one to six neurons, there was no clear association between the level of coupling and any functional component. Parasol cells from both groups of animals also displayed an inward rectifying or sag response, after the injection of hyperpolarizing current pulses.[30] Whereas the magnitude of the response was similar for the different populations of neurons (~2.5–15 mV), the response itself was threefold more prevalent in the normal (48%) versus glaucomatous (16%) parasol cells. A similar decrease in the frequency of the sag response has been noted in cat motoneurons after axotomy.[31]

Visual Response Properties

The visual response properties of each recorded neuron were examined by using randomly presented drifting and counterphased square-wave gratings that ranged spatially from 0.08 to 3.2 cyc/deg and were presented at 0.5 to 25 Hz temporal frequency. In the normal animals, approximately 52% of the cells displayed a clear doubling response and thus were classified as nonlinear. The proportion of nonlinear cells measured was slightly higher in the glaucomatous eyes (67%); however, this estimate most likely is inflated slightly by differences in the overall visual responsiveness of cells in the glaucomatous eyes. Although nearly all the parasol cells in the normal eyes were highly responsive to the grating stimuli (except the highly phasic neurons), many of the cells from the glaucomatous eyes either did not respond to the gratings, or responded only to full-field, nongrating, stimulation (Fig. 5). Parasol cells from both the normal and glaucomatous animals preferred gratings of low spatial frequency (0.08–0.2 cyc/deg), but differed with respect to their temporal response properties. The preferred temporal frequency of the glaucoma-related cells was approximately 4.8 Hz, whereas that of the normal cells was 6.6 Hz (Table 3; Fig. 6). In the normal cells, 64% (21/33; excluding the most phasic cells; e.g., Fig. 4A) were able to follow reliably the drift rates at least as high as

25 Hz, the highest rate that the image synthesizer could generate. In the glaucomatous eyes, only 41% of the pattern-responsive cells followed temporal frequencies of 16 Hz or greater, and only 27% were responded to the 25-Hz drifting grating. Extending the temporal frequency response curves of Figure 6 to the baseline results in estimates of maximum temporal responses of approximately 45 Hz for the normal cells and 35 Hz for those glaucomatous cells that responded to the grating.

A comparison of temporal frequency response functions obtained for four normal parasol cells and four parasol cells from glaucomatous eyes are presented in Figures 7 and 8. In general, all the temporal frequency response profiles are similar, in that they show high- and low-frequency attenuation. Despite their finer dendritic processes, the relatively normal appearing parasol cells in Figures 8A and 8B show temporal response characteristics similar to normal. These responses are much more attenuated, however, for the cells in Figures 8C and 8D, whose dendritic arbors are significantly more abnormal in size and complexity.

Discussion

The goal of this study was to examine the structural and functional characteristics of single ganglion cells in the glaucomatous primate eye. In agreement with our previous work, the data presented herein suggest that structural abnormalities related to the dendritic arbor are a primary feature of pressure-related ganglion cell degeneration.[11] These include not only changes in dendrite morphology and a decrease in dendritic field area, but also the loss of higher-order processes from more distal regions of the dendritic arbor. The overall result is a significant reduction in dendritic surface area, and thus, presumably, postsynaptic space and receptor integrity. That such changes can have functional consequences is suggested by the significant decrease in the number of parasol cells from the glaucomatous eyes that responded to visual stimulation, and in particular, patterned visual stimuli.

Although the biophysical properties of ganglion cells in the mammalian retina have been described previously in both slice and culture preparations, the work most relevant to the present study is that of O'Brien et al.,[30] in which they used a similar isolated retina preparation to compare the intrinsic response properties of ganglion cells in the adult feline retina. Despite considerable variability within each response category, the large α cells were readily distinguished by their mean input resistances and membrane time constants, which were at least four times lower than those of the other classes of ganglion cells studied (see Table 1 in O'Brien et al.[30]). In general, the biophysical characteristics of the α cells reported by O'Brien et al. are highly comparable to those of the parasol cells examined in the current study. This is not surprising, considering that these two classes of ganglion cells often are considered anatomically and functionally similar. The extent to which our lower estimates of input resistance for parasol cells (21.7 MΩ vs. 31.3 MΩ) might reflect real, methodological (whole-cell patch versus sharp electrode), or sampling differences, requires further investigation. Preparation quality may also be a factor; however, this explanation seems unlikely based on the good membrane resting potentials, low activation thresholds, large amplitude spikes, and, in normal cells, strong visual responses. Although O'Brien et al. report membrane time constants for their α cells that are approximately 67% longer than those obtained for our parasol cells (4.5 ms vs. 2.7 ms), it is important to note that they considered their time constant estimate to be an overestimate, because they excluded the fastest cells from their analysis. We did not, as the time course of the intracellular responses (1–4 ms) of these neurons were clearly different from the extracellular responses of the electrode alone (100–200 μs). O'Brien et al. also reported significantly higher spike frequencies for their α cells in response to electrical stimulation (262 Hz vs. 108 Hz); however, they used a depolarizing current level that was approximately twice that used in the present study (1.8 nA vs. 1.0 nA). Our decision to limit the maximum level of stimulation to 1.0 nA was based on our initial experience that parasol

cells from glaucomatous eyes often did not hold up well to electrical stimulation above 1.2 nA. Another factor affecting our spike-frequency measurements was the finding that not all parasol cells responded equally to depolarizing current pulses. Some produced only one to two spikes regardless of the level of depolarization; others started slowly, but quickly increased their rate of firing with increased stimulus intensity; and a third group of cells showed a high level of activity, even at the lowest levels of stimulation, and increased rapidly from there. Although we did not include the most phasic cells in our computations of spike frequency, we also did not restrict our estimates to only those with the highest firing rates, thus reducing the mean rate. One clear difference in the biophysical response properties of our parasol cells and the α cells examined by O'Brien et al., was the presence of a sag response, or anomalous rectification, in about half the normal parasol cells studied. Although this response also was seen in many of the other classes of feline ganglion cells, it was not a prominent feature of α cells, suggesting that ganglion cells differ with respect to the type and number of potassium channels they possess. At present, the role this hyperpolarizing-activated current plays in retinal function remains unknown. It appears, however, that the ion channels underlying this response are susceptible to the effects of glaucomatous neuropathy, as only one third of the parasol cells examined in the glaucomatous eyes displayed sag responses compared with normal.

Parasol cells in the normal eyes responded best to gratings of low spatial frequency, drifting at 8 to 10 Hz. When the temporal frequency response functions, which were limited to a maximum of 25 Hz by the pattern generator, were extended to the baseline, the projected temporal cutoff frequency for these neurons was approximately 45 Hz. Although the temporal response functions were similar in shape to those derived in vivo (i.e., band-pass), the peak temporal frequencies of the parasol cells examined by us were only approximately one half that reported previously.[32] This most likely reflects the significant reduction in image brightness imposed by presenting the visual stimuli through the microscope camera port and 40× objective (40 cd/m^2 at video monitor vs. 1 cd/m^2 at retina) and not our use of an isolated retina preparation. Previous studies have shown that decreasing stimulus luminance and contrast results in a shift of the temporal frequency response function toward lower optimal frequencies and response magnitudes.[20,21,32] Although we may have reduced this effect by using a lower-power objective (e.g., 4×), it was our experience that switching back and forth between the 40× water immersion and a dry objective often resulted in loss of the targeted cell. In addition, visual responsiveness is highly sensitive to focal quality at the tissue level, and this is monitored most reliably with the higher-power objective. The reduction in retinal luminance also guided our basis for focusing on the visual responses of parasol cells, whose sensitivities to luminance contrast are 8 to 10 times greater than those of midget ganglion cells.[20,21,32]

In a previous study, Smith et al.[33] used the primate model of glaucoma to examine, in vivo, the visual response properties of retinal target neurons in the dorsal lateral geniculate nucleus (LGN), after long-term (20–52 months) elevation of IOP. They concluded that visual deficits in long-term glaucoma result primarily from ganglion cell loss and not a reduction in the functional capacity of surviving neurons. Although the results of the present study appear to contradict this conclusion, there are several important differences between these two studies. First, many of the magnocellular LGN neurons sampled by Smith et al.[33] had receptive fields, and thus received their retinal input, from parasol cells located near central retina (0–15°). By contrast, because of the limited number of cells that could be studied per eye intracellularly, we restricted our retinal sampling to mid-temporal retina (15–30°), the region considered clinically to be most vulnerable to glaucoma-related injury[17–19]; ganglion cells located in these regions give rise to the arcuate fibers that form the superior and inferior poles of the optic nerve head, regions shown to be affected most often in glaucomatous eyes.[17–19] In this respect, it is important to note that Smith et al.,[33] reported their greatest reductions in retinal innervation were associated with LGN receptive field locations outside the macular region, but in regions

associated with the arcuate fibers. Thus, it is likely that some of the differences between these two studies result from differences in the locations of the retinal cells targeted. Second, except for animals with higher mean levels of IOP (37–53 mm Hg vs. 23–53 mm Hg; Smith et al.), the changes in cup-disc ratio for most of the animals examined by Smith et al.[33] were more modest (0.2–0.4) than those determined for the animals used in our study (0.4–0.9), suggesting that the eyes of our animals had experienced, on average, a more significant level of degeneration. Of note, these investigators state that in three animals with severe nerve damage, they were able to drive only 20/194 units encountered through the glaucomatous eye and that, in many passes, they were unable to drive any cells by the affected eye. Although they ascribe this to a loss of retinal ganglion cell innervation to this region of the LGN, it also is possible that, to some extent, these silent regions represent areas of the nucleus that continue to receive retinal input, but that the ganglion cells providing the input no longer respond normally to the visual stimuli used. This could form the basis for the LGN neurons they encountered that showed spontaneous activity, but could not be influenced by visual stimulation. An interesting comparison would have been the relation between the location and encounter rate of LGN neurons determined physiologically and that derived from the histologic reconstructions of Smith et al.[33] A third factor that may have contributed to the different conclusions of these two studies is the method of cell sampling. In the approach used by Smith et al. the LGN neurons, and thus the retinal afferents, analyzed were identified by their ability to respond to presentation of a visual stimulus. This may have caused a bias toward those cells that retained relatively normal levels of retinal innervation. By contrast, the retinal neurons in the present study were selected randomly through direct visualization, thus removing any functional bias from the selection process. Finally, it is important to note the different time frames of the two studies. The animals examined by Smith et al. had their IOP elevated by laser treatment,[34–36] then received little additional intervention over a 20- to 58-month survival period, during which IOP was allowed to decline slowly to normal. The animals in this study had their IOP elevated by repeated (sometimes biweekly) intraocular injections of latex microspheres.[14] While these injections were moderated carefully so as not to induce acute spikes in IOP, we did see a higher frequency, although not necessarily higher magnitude, of fluctuations in IOP in our animals compared with those of Smith et al. (see their Fig. 1 in Ref. 33). Furthermore, the IOPs of the animals used in our study were not reduced to normal (~16 mm Hg) until 24 to 48 hours before examination of the retina. As noted by Smith et al., it is possible that their data reflect a system that has stabilized with time, whereas the results of the present study more closely reflect short-term changes in retinal function. Thus, while the data presented herein do not refute the conclusion of Smith et al., that visual deficits in glaucoma result primarily from ganglion cell loss, they do indicate that abnormal visual function by surviving ganglion cells also must be considered a contributing factor.

Regardless the mechanism underlying visual dysfunction, it is important to note that many of the glaucoma-related ganglion cells showed a high degree of normalcy in their intrinsic membrane properties, suggesting that, despite relatively significant changes in morphology, their cell membranes are basically intact. This is not surprising, considering the wide range of effects seen with respect to the intrinsic membrane properties of neurons from other systems after axonal injury.[37] The extent to which this may represent a resistance to injury by these neurons is difficult to assess, since glaucomatous changes typically are not uniform across the retina, spatially or in degree.[38,39] Although it was our intent that by combining the intracellular recording and labeling techniques we would be able to identify a specific structure-function deficit in the glaucomatous eyes, no such relation was obvious. The decreased spatial–temporal responsiveness of ganglion cells from these animals appears to result from global changes in dendritic structure, which then have a negative impact on synaptic integrity. Variations among degenerating neurons most likely reflect complex differences in the number, type, and distribution of synaptic inputs along the dendrites of different neurons,[40,41] their differential

influences on the response properties of those cells, and the spatial–temporal pattern of degeneration induced by the disease.

Thus, the data presented here suggest that decreases in the spatial–temporal response properties of single ganglion cells contribute to the spatial and temporal deficits identified psychophysically in glaucoma.[42–51] These functional deficits most likely derive from pressure-induced changes in the structural integrity and synaptic organization of the affected neurons, but not necessarily changes in their intrinsic neuronal membrane properties.

Acknowledgements

The authors thank Michael Bueche for assistance with clinical evaluations of the eyes and Judy McMillan for technical assistance.

References

1. Morgan JE, Jeffery G, Foss AJ. Axon deviation in the human lamina cribrosa. Br J Ophthalmol 1998;82:680–683. [PubMed: 9797672]
2. Findl O, Strenn K, Woltz M, et al. Effects of changes in intraocular pressure on human ocular haemodynamics. Curr Eye Res 1997;16:1024–1029. [PubMed: 9330854]
3. Pillunat LE, Anderson DR, Knighton RW, Joos KM, Feuer WJ. Autoregulation of human optic nerve head circulation in response to increased intraocular pressure. Exp Eye Res 1997;64:737–744. [PubMed: 9245904]
4. Harris A, Ciulla TA, Chung HS, Martin B. Regulation of retinal and optic nerve blood flow. Arch Ophthalmol 1998;116:1491–1495. [PubMed: 9823351]
5. Neufeld AH, Hernandez MR, Gonzalez M. Nitric oxide synthase in the human glaucomatous optic nerve head. Arch Ophthalmol 1997;115:497–503. [PubMed: 9109759]
6. Tezel G, Wax MB. Increased production of tumor necrosis factor-alpha by glial cells exposed to simulated ischemia or elevated hydrostatic pressure induces apoptosis in co-cultured retinal ganglion cells. J Neurosci 2000;20:8693–8700. [PubMed: 11102475]
7. Yuan L, Neufeld AH. Tumor necrosis factor-alpha: a potentially neurodestructive cytokine produces by glia in the human glaucomatous optic nerve head. Glia 2000;32:42–50. [PubMed: 10975909]
8. Nickells RW. Retinal ganglion cell death in glaucoma: the how, the why, and the maybe. J Glaucoma 1996;5:345–356. [PubMed: 8897235]
9. Morgan JE. Selective cell death in glaucoma: does it really occur? Br J Ophthalmol 1994;78:875–879. [PubMed: 7848987]
10. Quigley HA. Open-angle glaucoma. N Engl J Med 1993;328:1097–1106. [PubMed: 8455668]
11. Weber AJ, Kaufman PL, Hubbard WC, Stanford LR. Morphology of single ganglion cells in the glaucomatous primate retina. Invest Ophthalmol Vis Sci 1998;39:2304–2320. [PubMed: 9804139]
12. Dowling JE. *The Retina: an Approachable Part of the Brain.* Cambridge, MA: Belknap Press; 1987;12–123.
13. Rodieck RW. *The First Steps in Seeing.* Sunderland, MA: Sinauer, 1998;255–265.
14. Weber AJ, Zelenak D. Experimental glaucoma in the primate induced by latex microspheres. Invest Ophthalmol Vis Sci 2001;111:39–48.
15. Saito AH. Morphology of physiologically identified X-, Y-, and W-type retinal ganglion cells of the cat. J Comp Neurol 1983;221:279–288. [PubMed: 6655086]
16. Kaplan E, Lee BB, Shapley RM. New views of primate retinal function. In: Osborne N, Chader G, eds. *Progress in Retinal Research.* Oxford, UK: Pergamon; 1990;273–336.
17. Quigley HA, Addicks EM. Regional differences in the structure of the lamina cribrosa and their relation to glaucomatous optic nerve damage. Arch Ophthalmol 1981;99:137–143. [PubMed: 7458737]
18. Quigley HA, Addicks EM, Green WR. Optic nerve damage in human glaucoma. III. Quantitative correlation of nerve fiber loss and visual field defect in glaucoma, ischemic neuropathy, papilledema, and toxic neuropathy. Arch Ophthalmol 1982;100:135–146. [PubMed: 7055464]

19. Heijl A. Visual field loss and perimetry in glaucoma. In: Podos SM, Yanoff M, Kaufman PL, Mittag TW, eds. *Glaucoma.* London, Mosby; 1994:7.6–7.27; *Textbook of Ophthalmology*; vol. 7.
20. Lee BB. Receptive field structure in the primate retina. Vision Res 1996;36:631–644. [PubMed: 8762295]
21. Kaplan E, Benardete E. The dynamics of primate retinal ganglion cells. Prog Brain Res 2001;134:17–34. [PubMed: 11702542]
22. Quigley HA, Sanchez RM, Dunkelberger GR, L'Hernault NL, Baginski TA. Chronic glaucoma selectively damages large optic nerve fibers. Invest Ophthalmol Vis Sci 1987;28:913–920. [PubMed: 3583630]
23. Glovinsky Y, Quigley HA, Dunkelberger GR. Retinal ganglion cell loss is size dependent in experimental glaucoma. Invest Ophthalmol Visual Sci 1991;32:484–490. [PubMed: 2001923]
24. Weber AJ, Chen H, Hubbard WC, Kaufman PL. Experimental glaucoma and cell size, density, and number in the primate lateral geniculate nucleus (LGN). Invest Ophthalmol Vis Sci 2000;41:1370–1379. [PubMed: 10798652]
25. Rodieck RW, Binmoeller KF, Dineen J. Parasol and midget ganglion cells of the human retina. J Comp Neurol 1985;233:115–132. [PubMed: 3980768]
26. Dacey D, Petersen MR. Dendritic field size and morphology of midget and parasol ganglion cells in the human retina. Proc Natl Acad Sci USA 1992;89:9666–9670. [PubMed: 1409680]
27. Kolb H, Linberg KA, Fisher SK. Neurons of the human retina: a Golgi study. J Comp Neurol 1992;318:147–187. [PubMed: 1374766]
28. Watanabe M, Rodieck RW. Parasol and midget ganglion cells of the primate retina. J Comp Neurol 1989;289:434–454. [PubMed: 2808778]
29. Sholl DA. Dendritic organization in the neurons of the visual and motor cortices of the cat. J Anat (Lond) 1953;87:387–406. [PubMed: 13117757]
30. O'Brien BJ, Isayama T, Richardson R, Berson DM. Intrinsic physiologic properties of cat retinal ganglion cells. J Physiol 2002;538:787–802. [PubMed: 11826165]
31. Gustafsson B, Pinter MJ. Factors determining the variation of the afterhyperpolarization duration in cat lumbar α-motorneurones. Brain Res 1985;326:392–395. [PubMed: 3971165]
32. Kelly DH. Visual responses to time-dependent stimuli. I. Amplitude sensitivity measurements. J Opt Soc Am 1961;51:422–429. [PubMed: 13752375]
33. Smith EL III, Chino YM, Harwerth RS, Ridder WH III, Crawford MLJ, DeSantis L. Retinal inputs to the monkey lateral geniculate nucleus in experimental glaucoma. Clin Vis Sci 1993;8:113–139.
34. Pederson JE, Gaasterland DE. Laser-induced primate glaucoma. I. Progression of cupping. Arch Ophthalmol 1984;102:1689–1692. [PubMed: 6541902]
35. Gaasterland DE, Kupfer C. Experimental glaucoma in the rhesus monkey. Invest Ophthalmol 1974;13:455–457. [PubMed: 4208801]
36. Quigley HA, Hohman RM. Laser energy levels for trabecular mesh-work damage in the primate eye. Invest Ophthalmol Vis Sci 1983;24:1305–1307. [PubMed: 6885314]
37. Titmus MJ, Faber DS. Axotomy-induced alterations in the electro-physiological characteristics of neurons. Prog Neurobiol 1990;35:1–51. [PubMed: 2217820]
38. Quigley HA, Dunkelberger GR, Green WR. Retinal ganglion cell atrophy correlated with automated perimetry in human eyes with glaucoma. Am J Ophthalmol 1989;107:453–464. [PubMed: 2712129]
39. Airaksinen PJ, Drance SM, Douglas GR. Diffuse and localized nerve fiber loss in glaucoma. Am J Ophthalmol 1984;98:566–571. [PubMed: 6496612]
40. Weber AJ, McCall MA, Stanford LR. Synaptic inputs to physiologically identified retinal X-cells in the cat. J Comp Neurol 1991;314:350–366. [PubMed: 1787179]
41. Weber AJ, Stanford LR. Synaptology of physiologically identified ganglion cells in the cat retina: a comparison of retinal X- and Y-cells. J Comp Neurol 1994;343:483–499. [PubMed: 8027453]
42. Johnson CA. Early losses of visual function in glaucoma. Optometry Vis Sci 1995;72:359–370.
43. Casson EJ, Johnson CA. Temporal modulation perimetry in glaucoma and ocular hypertension. In: Mill RP, Heijl A, eds. *Perimetry Update 1992/1993* Amsterdam: Kugler, 1993:443–450.
44. Bosworth CF, Sample PA, Weinreb RN. Motion perception thresholds in area of glaucomatous visual field loss. Vision Res 1997;37:355–364. [PubMed: 9135868]

45. Bosworth CF, Sample PA, Weinreb RN. Perimetric motion thresholds are elevated in primary open angle glaucoma patients. Vision Res 1997;37:1989–1997. [PubMed: 9274783]

46. Trick GL, Steinman BS, Amyot M. Motion perception deficits in glaucomatous optic neuropathy. Vision Res 1995;25:2225–2233. [PubMed: 7667933]

47. Silverman SE, Trick GL, Hart WM Jr. Motion perception is abnormal in primary open angle glaucoma. Invest Ophthalmol Vis Sci 1990;31:722–729. [PubMed: 2335439]

48. Sample PA, Bosworth CF, Weinreb RN. Short-wavelength automated perimetry and motion automated perimetry in patients with glaucoma. Arch Ophthalmol 1997;115:1129–1133. [PubMed: 9298053]

49. Johnson CA, Samuels SJ. Screening for glaucomatous visual field loss with frequency-doubling perimetry. Invest Ophthalmol Vis Sci 1997;38:413–425. [PubMed: 9040475]

50. Kelly DH. Frequency doubling in visual responses. J Opt Soc Am 1966;56:1628–1633.

51. Kelly DH. Nonlinear visual responses to flickering sinusoidal gratings. J Opt Soc Am 1981;71:1051–1055. [PubMed: 7277060]

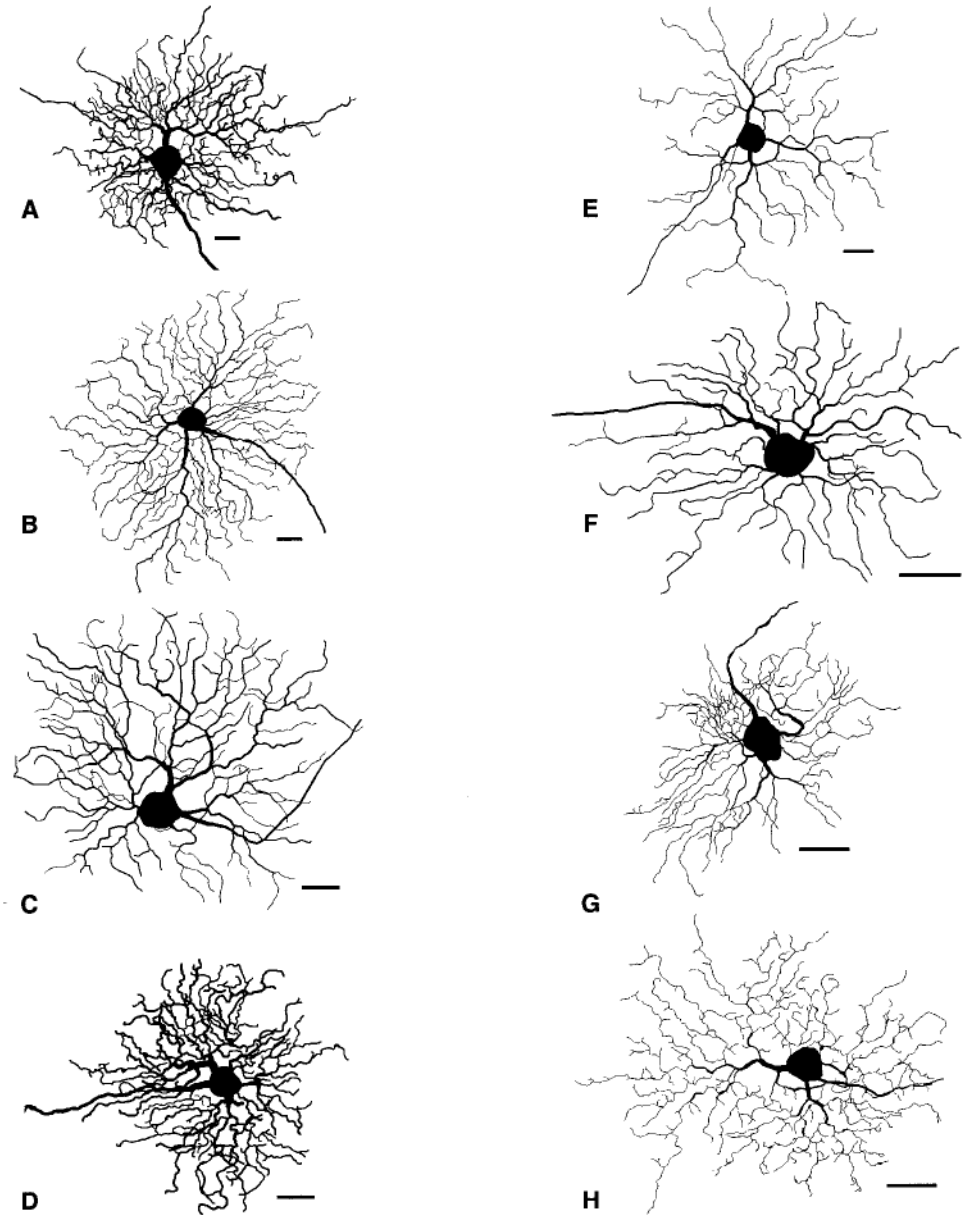

Figure 1.
Morphologic comparison of parasol cells from normal (**A**–**D**) and glaucomatous (**E**–**H**) eyes that were labeled intracellularly and reconstructed. A prominent difference is the reduced thickness and complexity of the dendritic arbors of the glaucomatous cells. Scale bars, 25 μm.

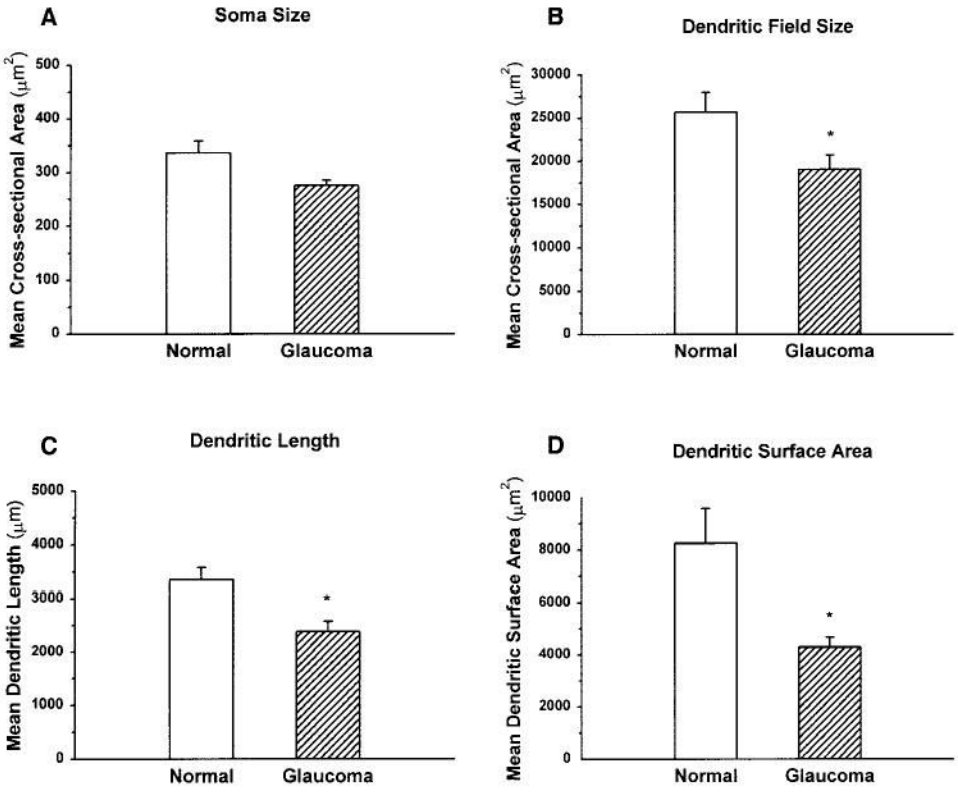

Figure 2.

Comparisons of the differences in mean soma size (**A**), dendrite field area (**B**), dendrite length (**C**), and dendrite surface area (**D**) of parasol cells recovered from normal and glaucomatous eyes. *$P < 0.05$.

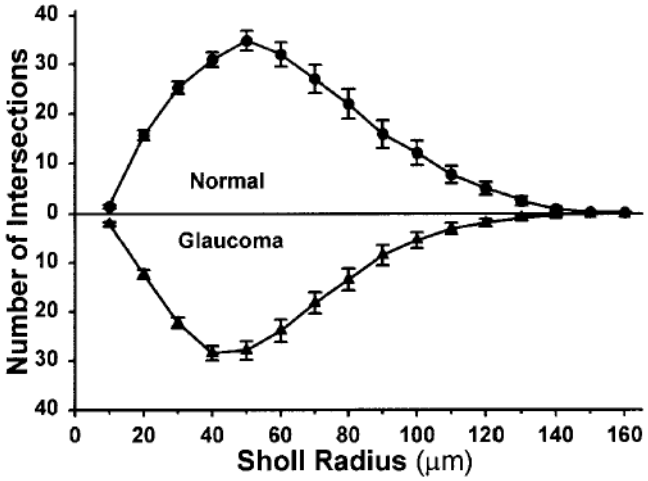

Figure 3.
Sholl analysis comparing the dendritic complexities of normal and glaucomatous parasol cells based on differences in the mean number of profile intersections. The leftward shift for the glaucomatous animals reflects changes associated with more peripheral dendritic regions. Sphere resolution, 10 μm.

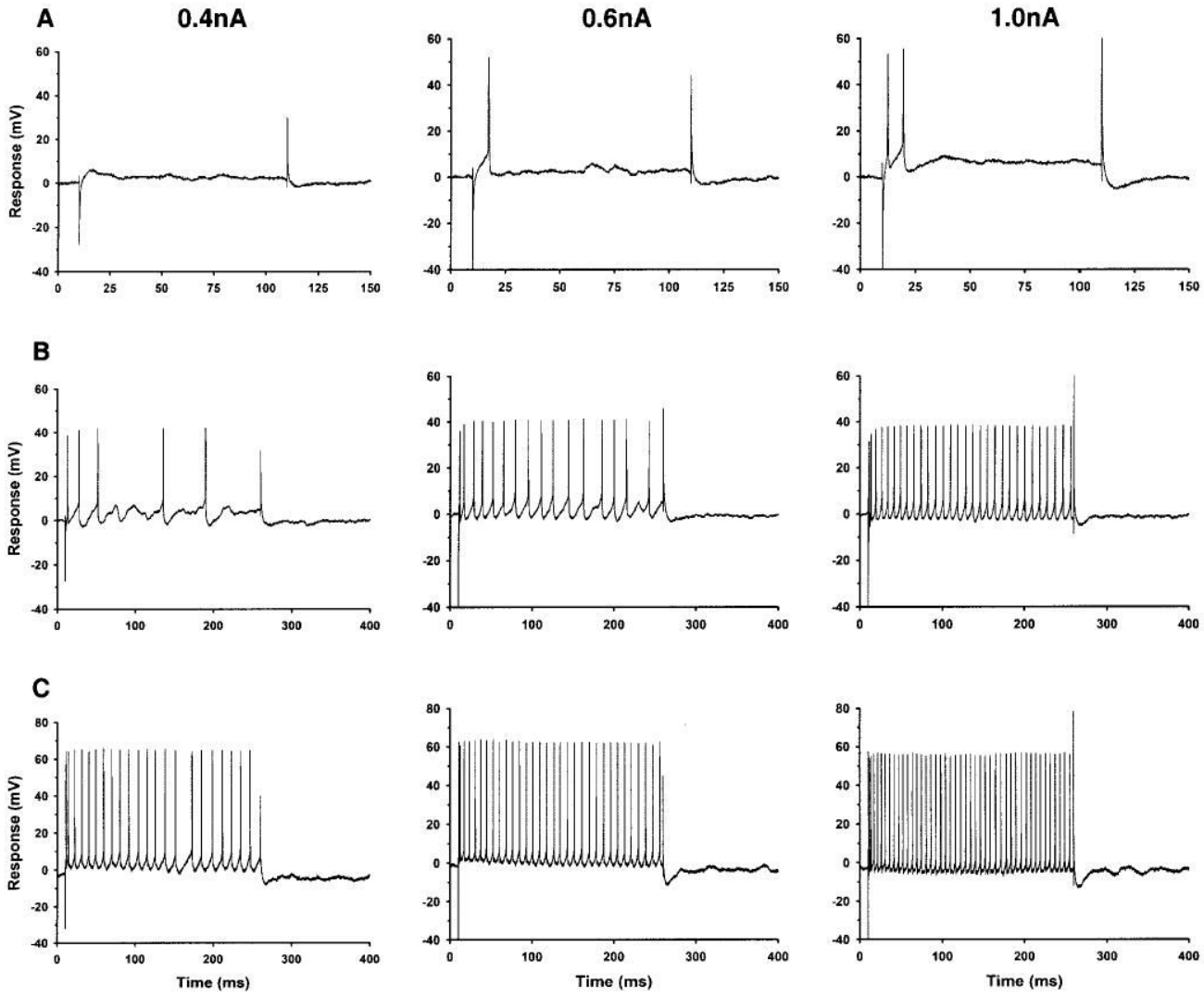

Figure 4.

Parasol cells from both groups of animals showed three distinct patterns of activity in response to electrical stimulation. Those in category (**A**) were extremely phasic, regardless of the level of stimulation, whereas those in categories (**B**) and (**C**) showed progressively greater levels of activation at each level of stimulation.

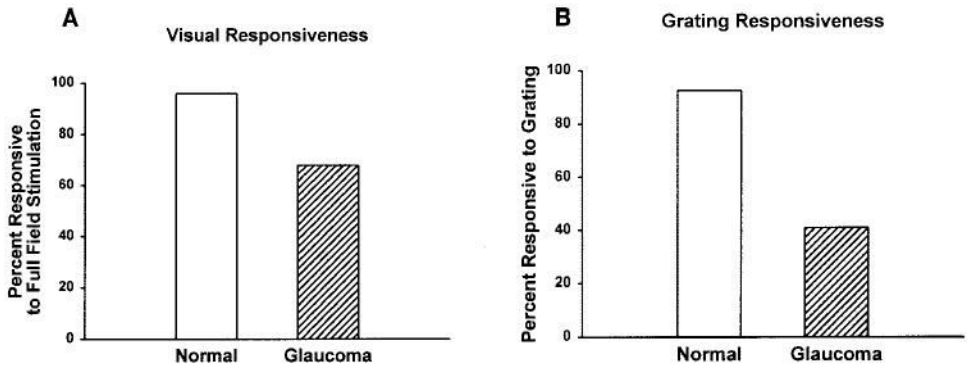

Figure 5.
A major difference between normal and glaucomatous cells was the decreased ability of the latter to respond to visual stimuli (**A**), and in particular, patterned visual stimuli (**B**).

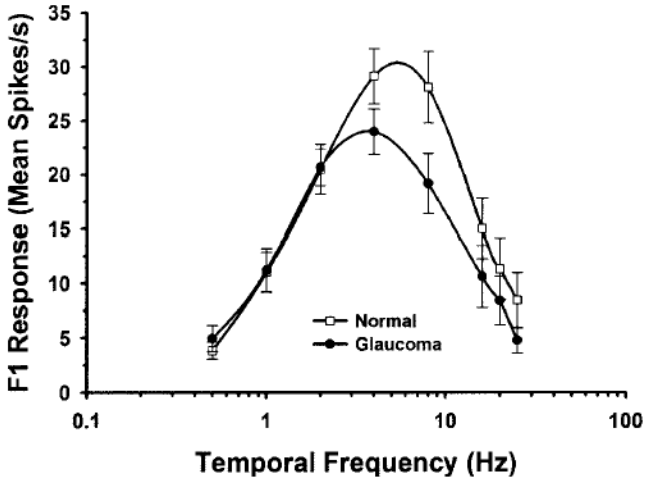

Figure 6.
Parasol cells from glaucomatous eyes displayed not only reduced spatial responsiveness, but also significant differences in their ability to follow stimuli of increased temporal frequency ($P < 0.05$).

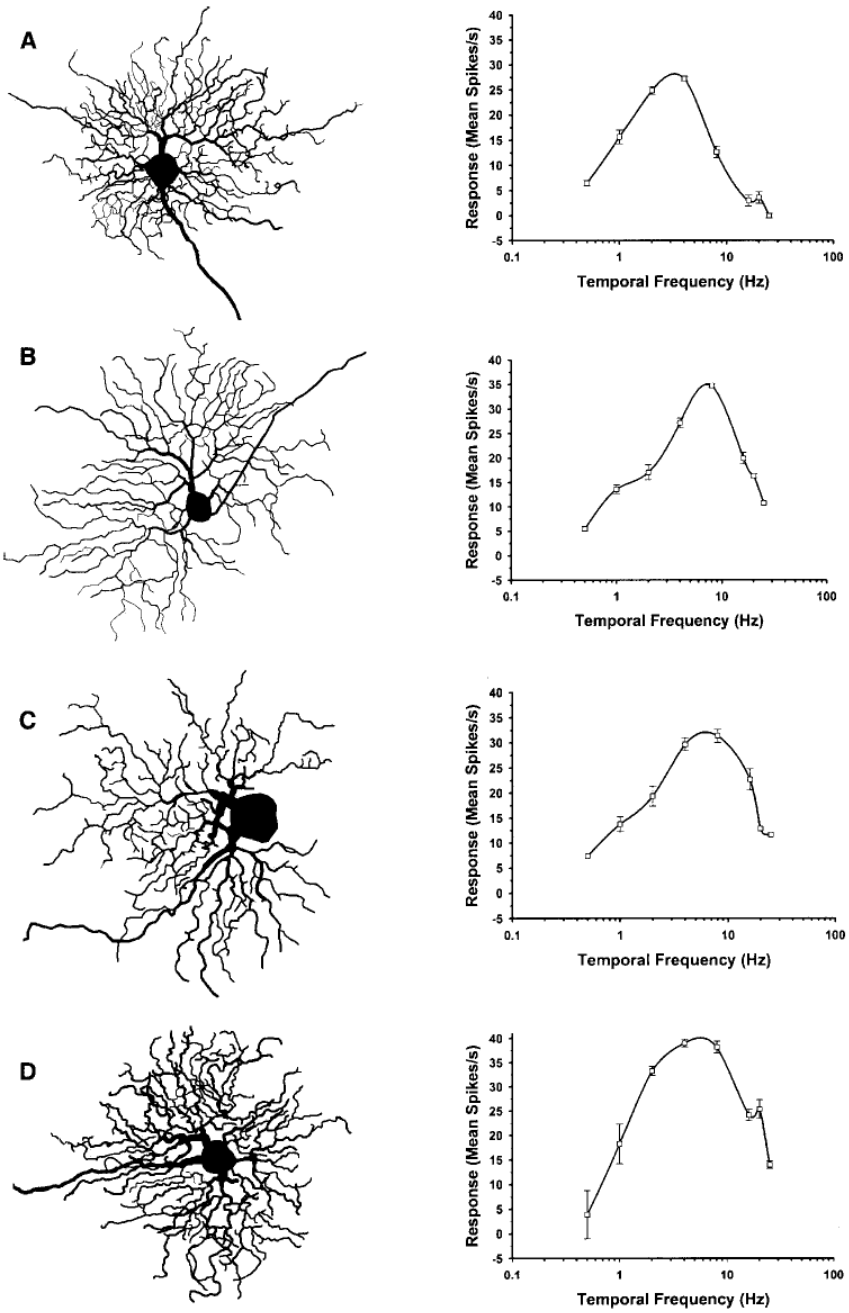

Figure 7.
Temporal frequency response functions of four normal parasol cells (**A**–**D**). The responses show high- and low-frequency attenuation, with peak responses in the range of 35 to 40 spikes/s.

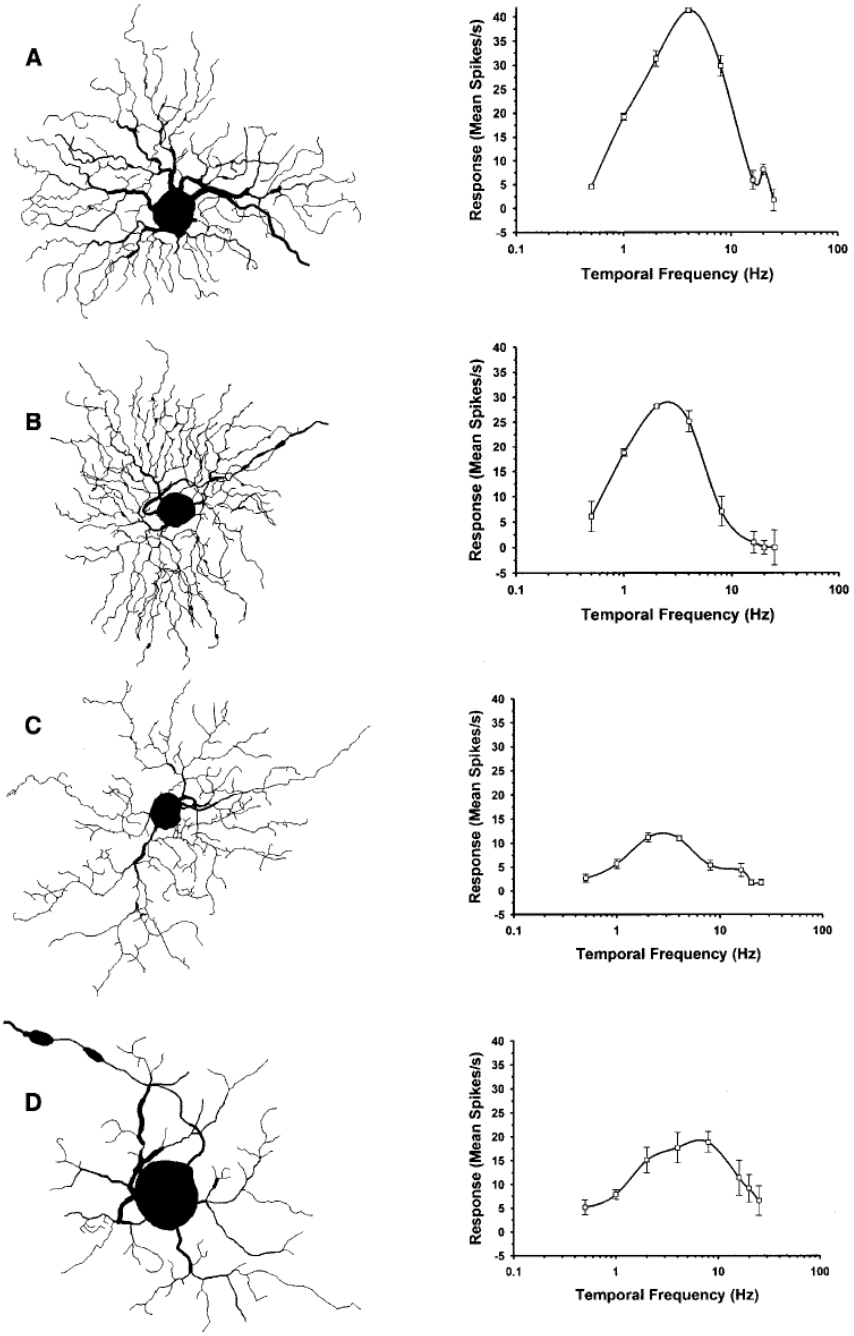

Figure 8.

Temporal frequency response functions of four cells (**A**–**D**) of glaucomatous eyes that showed progressive signs of degeneration, morphologically. As in normal cells, the responses were band-pass; however, the response amplitude diminished with loss of dendritic complexity.

Table 1

IOP Data for Animals with Experimental Glaucoma

Animal	Mean IOP (mm Hg)	Peak IOP (mm Hg)	Duration (wks)	C/D Ratio* (initial/final)
M762	32.3 ± 15.5	60	18	0.3/0.8
M9253	32.9 ± 15.2	57	18	0.2/0.7
M9186	29.5 ± 9.9	49	18	0.2/0.5
M3648	41.7 ± 16.2	72	18	0.2/0.6
AQ97	28.7 ± 7.7	49	19	0.2/0.7
R90119	27.6 ± 9.8	34	27	0.2/0.5
M65-117	34.4 ± 14.6	61	28	0.2/0.7
M6576	31.9 ± 9.2	45	35	0.2/0.5
AR86	27.6 ± 9.8	48	34	0.2/0.5
AR12	32.0 ± 11.1	60	35	0.2/0.7
M3260	25.0 ± 12.2	47	35	0.2/0.4
M7490	33.9 ± 8.8	49	35	0.3/0.6
M3903	34.0 ± 16.5	72	36	0.2/0.9
M2654	36.5 ± 9.9	60	120	0.2/0.8
M1854	36.2 ± 12.3	64	144	0.2/0.8

C/D cup-to-disc ratio.

* Based on OD contour with IOP reduced to normal (≈16 mm Hg)

Table 2

Summary of Morphologic Features

	Soma Area (μm^2)	Soma Surface Area (μm^2)	Dendritic Field Area (μm^2)	Number of Dendrites	Sholl Analysis Intersections	Dendritic Length (μm)	Dendritic Surface Area (μm^2)	Total Surface Area (μm^2)	Total Volume (μm^3)
Normal									
Mean	336.66	1,354.24	25,671.37	223.60	234.20	3,352.58	8,247.37	9,601.62	1,875.93
SE	21.89	87.28	2,302.21	16.06	18.01	224.60	1,329.59	1,391.97	350.74
n	29	29	29	29	29	29	29	29	29
Glaucoma									
Mean	276.11	1,104.34	19,059.50	175.80	168.30	2,381.12	4,294.10	5,398.44	948.13
SE	9.93	39.74	1,701.41	15.45	13.41	198.38	392.30	398.40	95.98
n	36	36	36	36	36	36	36	36	36
% Different	18.0	18.5	25.8*	21.4	28.1*	29.0*	47.9*	43.8*	49.5*

*$P < 0.05$, Mann-Whitney.

Table 3

Summary of Physiological Characteristics

	RP (mV)	Rn (MΩ)	τm (ms)	Threshold (nA)	Spike Amp (mV)	Spike Width at Half Height	Max. Rate (spikes/s)	Best SF (c/cm)	Best TF (Hz)
Normal									
Mean	−53.03	21.73	2.69	0.31	45.20	0.43	108.1	0.22	6.56
SE	0.68	1.49	0.14	0.04	1.15	0.02	8.21	0.03	0.73
n	61	61	61	61	61	61	61	41	42
Glaucoma									
Mean	−53.98	22.53	2.20	0.33	46.35	0.50	92.81	0.20	4.79
SE	1.25	1.87	0.12	0.05	1.78	0.02	9.77	0.01	0.67
n	36	36	36	36	36	36	36	25	25
% Difference	1.7	3.7	18.5*	6.5	2.7	25.0*	14.9	9.1	31.8†

RP, resting potential; SF, spatial frequency; TF, temporal frequency.

* $P < 0.05$, Mann-Whitney.

† $P < 0.05$, Student's *t*-test.